

All oxide thermoelectric devices: Comparison between conventional and “unileg” architecture.

S. Lemonnier, C. Goupil, J. Noudem and E. Guilmeau

*Laboratoire CRISMAT, UMR CNRS ENSICAEN 6508
6 Bd Maréchal Juin, 14050 CAEN cedex
sebastien.lemonnier@ensicaen.fr*

Abstract.

We report the design, realization and complete characterization of oxide thermoelectric generators. Two different architectures have been developed. The first one is a classical design using two types of oxides, respectively $\text{Ca}_{0.95}\text{Sm}_{0.05}\text{MnO}_3$ (N-type) and $\text{Ca}_3\text{Co}_4\text{O}_9$ (P-type), while the second and third ones are only composed of one type of material, respectively $\text{Ca}_{0.95}\text{Sm}_{0.05}\text{MnO}_3$ (N-type) and $\text{In}_{1.94}\text{Ge}_{0.06}\text{O}_3$ (N-type), so called “unileg type devices”. While this latter seems to be less efficient, in term of electrical generation than the classical P-N geometry, it benefits from the use of a unique material involved in the device. This point is of importance for large temperature applications where the various differential dilatations of the P and N materials contribute to strongly reduce the reliability of the final devices.

Introduction

Thermoelectricity has recently been the subject of numerous studies motivated by the energy cost reduction and environmental protection. The thermoelectric device performances are governed by materials intrinsic factors including Seebeck coefficient α ($\mu\text{V}/\text{K}$), electrical resistivity ρ ($\text{m}\Omega\cdot\text{cm}$) and thermal conductivity κ (W/Km) and extrinsic factors, like leg geometry, electric and thermal contacts. Since oxide materials present good stability in air at high temperature, and do not contain harmful or volatilizing elements, these materials are considered to be serious candidates for high temperatures thermoelectric applications. Furthermore, the thermoelectric figures-of-merit ZT of new

oxides let envisage promising applications [1-4]. More especially, the N-type CaMnO_3 [5], Ge-doped In_2O_3 [6] and P-type $\text{Ca}_3\text{Co}_4\text{O}_9$ [7] phases show promising properties. However, only a few papers deal with the fabrication and the characterization of oxide-based thermoelectric devices [8-14].

These three cited compounds were integrated in thermoelectric devices using Ag paste and foils, and the modules were annealed at 920°C for 2 hours in air. The devices have been characterized under large temperature difference, $\Delta T \approx 200\text{--}500$ K with a hot source temperature varying from 660 K to 900 K. The P-N and unileg geometries are compared in term of electrical generation performances.

Experimental procedure

The three compounds were prepared by solid state reaction. The n-type $\text{Ca}_{0.95}\text{Sm}_{0.05}\text{MnO}_3$ samples were synthesized, mixing CaCO_3 , MnO_2 and Sm_2O_3 in stoichiometric proportions. The powders were calcinated at 900°C for 24 hours in air and then pressed into pellets (24mm in diameter) by uniaxial press (with a load of 9.5 MPa). The samples were sintered at 1350°C for 30 minutes in air, with heating and cooling rates of $150^\circ\text{C}/\text{h}$. The $\text{Ca}_3\text{Co}_4\text{O}_9$ samples were synthesized following the same scheme with CaCO_3 and CoO_2 as precursors with a similar calcination treatment but a sintering at 920°C for 24h. The $\text{In}_{1.94}\text{Ge}_{0.06}\text{O}_3$ compound was obtained using In_2O_3 and GeO_2 precursors and a unique heat treatment at 1300°C for 48h. The sintered bars were cut for further use in module fabrication. The X-ray diffraction pattern,

carried out on a X'pert diffractometer did not reveal any secondary phases except for the $\text{In}_{1.94}\text{Ge}_{0.06}\text{O}_3$ compound which present $\text{In}_2\text{Ge}_2\text{O}_7$ impurities (composite material [6]). The nominal compositions were also confirmed by EDS (Electron Diffraction Spectroscopy) analyses (EDAX) using a SUPRA 55 SEM (ZEISS) apparatus. Thermoelectric properties, as electrical resistivity ρ ($\text{m}\Omega\cdot\text{cm}$), and Seebeck coefficient S ($\mu\text{V}/\text{K}$), were carried out from 300K to 1000K using a ZEM-3 apparatus (ULVAC-RIKO).

Three thermoelectric modules have been built using silver paste as bonding agent (4929N Dupont) between the silver strips (1mm in thickness) and the elements. The whole system was glued with silver paste between two alumina plates of $25*25*1.5 \text{ mm}^3$ used as electric insulators from the hot and cold sources. The devices were then annealed at 920°C for 2 hours in air to remove Ag-paste solvent and improve the electric contacts. The photographs of the two devices are given in figure 1.

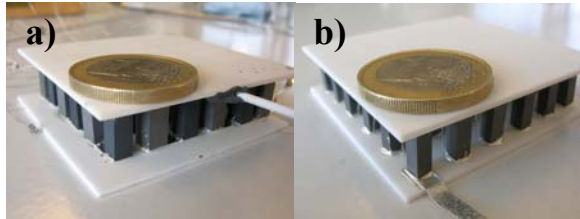


Figure 1: Photographies of a) the PN module and b) the $\text{Ca}_{0.95}\text{Sm}_{0.05}\text{MnO}_3$ -based unileg module.

The modules were tested under large temperature difference. The top alumina plate is heated with mica heaters at T_{hot} (hot temperature), whereas the bottom alumina plate is kept at T_{cold} (cold temperature), by using a water cooled copper block. The thermoelectric device temperatures were measured using two k-type thermocouples stuck on alumina plates with refractory cement. Five measurements were carried out using different electrical loads corresponding to open circuit, short circuit and close circuit configurations. The first measurement is used to have the direct measurement of the

open voltage E_0 at the output of the thermoelectric device. The others, under “closed” circuit conditions, were performed using electrical loads R_L of 1, 2 and 3 Ω and short circuit, and allow measuring the output voltage V_{out} and the output current I_{out} (A) values. These parameters are recorded for each electrical load with the same temperature difference ΔT through a Keithley-K2700/7700 system.

The theoretical internal resistance R_{ideal} of the device corresponding to the sum of the bars resistances is different from the real case due to the electrical contact resistances R_{contact} between the oxide and the metal. So the real module internal resistance R_{int} is in fact given by the relation: $R_{\text{int}} = R_{\text{ideal}} + R_{\text{contact}}$.

Obviously, R_{contact} should be as low as possible in order to get a maximum output power P_{max} , defined as $P_{\text{max}} = \frac{E_0^2}{4 \times R_{\text{int}}}$, obtained for adapted load, i.e., $R_L = R_{\text{int}}$.

Results

The electrical resistivity and Seebeck coefficient versus temperature curves for P-type and N-type compounds are shown respectively in figures 2 and 3.

The three materials present a metallic behaviour at high temperature with a slight increase of ρ with temperature. The $\text{Ca}_{0.95}\text{Sm}_{0.05}\text{MnO}_3$ compound presents relatively low electrical resistivity which varies from 6.5 $\text{m}\Omega\cdot\text{cm}$ at 300 K to 13.4 $\text{m}\Omega\cdot\text{cm}$ at 1000 K. In the same time, the Seebeck coefficient increases from -130 $\mu\text{V}/\text{K}$ to -190 $\mu\text{V}/\text{K}$. With value of 45 $\text{m}\Omega\cdot\text{cm}$ at 1000 K, the electrical resistivity of the $\text{Ca}_3\text{Co}_4\text{O}_9$ compound is higher than those reported in the literature [15] due to the unused texturation/densification process. However, the synthesis method used in the present study allows obtaining bars with large volumes more suitable in the device conception. The Seebeck coefficient increases with temperature and reaches a

value $+175 \mu\text{V/K}$ at 850 K. For the third compound, $\text{In}_{1.94}\text{Ge}_{0.06}\text{O}_3$, the electrical resistivity is very low, with an increase from $0.8 \text{ m}\Omega\cdot\text{cm}$ at room temperature to $1.8 \text{ m}\Omega\cdot\text{cm}$ at 1000 K. In parallel, the Seebeck coefficient varies from $-55 \mu\text{V/K}$ at RT to $-116 \mu\text{V/K}$ at 1000 K. The comparison between the compounds shows the first interesting point of the unileg exotic architecture, since the use of $\text{Ca}_3\text{Co}_4\text{O}_9$ compound showing higher electrical resistivity can be avoided.

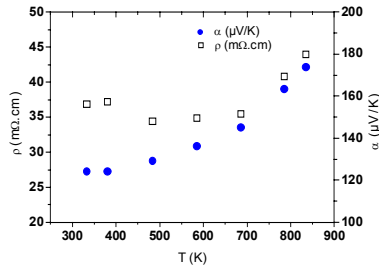


Figure 2: Temperature dependences of the electrical resistivity and Seebeck coefficient of the $\text{Ca}_3\text{Co}_4\text{O}_9$ compound.

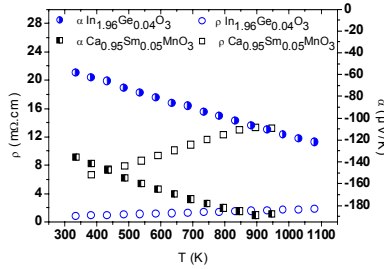


Figure 3: Temperature dependences of the electrical resistivity and Seebeck coefficient of the N-type compounds.

The output voltage E_0 measured, for the PN device in open circuit, reaches 2.62V for a ΔT value of 460 K and a T_{hot} temperature of 907 K. In the second device, the unileg $\text{Ca}_{0.95}\text{Sm}_{0.05}\text{MnO}_3$ -based, E_0 reaches 2.1 V with a ΔT value of 363 K and a T_{hot} temperature of 710 K. The $\text{In}_{1.94}\text{Ge}_{0.06}\text{O}_3$ -based unileg module presents a value of 0.240V with a ΔT value of 200 K and a T_{hot} temperature of 660 K. These values are very close to the theoretical ones, calculated with the relation $E_0 = 2N\langle S \rangle \Delta T$ (where N is half of the number of legs).

The devices were then measured in close circuit on electrical load using loads of 1, 2 and 3Ω and finally in short circuit. These

measurements give the internal resistance of the module R_{int} . The output voltage V_{out} , in close circuit on electrical load conditions, can be deduced by the relation $V_{out} = E_0(R_L / (R_{int} + R_L))$ and the output current I_{out} given by the relation $I_{out} = E_0 / (R_{int} + R_L)$. Plotting V_{out} versus I_{out} for the same module temperature difference, a linear straight is expected with slope equal to R_{int} and the origin ordinate equal to E_0 . The output power P_{out} can also be calculated. Figures 4, 5 and 6 show the results of the measurements carried out on the three devices.

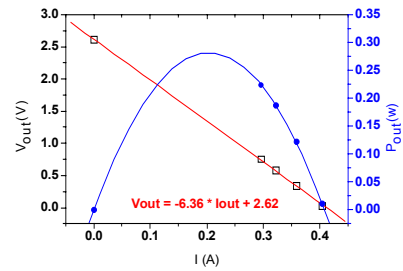


Figure 4: V_{out} versus I_{out} and P_{out} for the conventional PN module

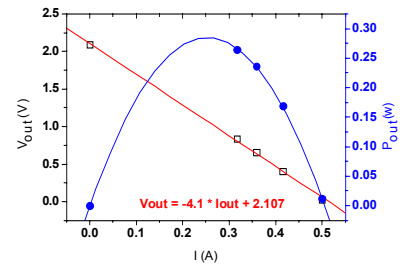


Figure 5: V_{out} versus I_{out} and P_{out} for the $\text{Ca}_{0.95}\text{Sm}_{0.05}\text{MnO}_3$ -based unileg type device

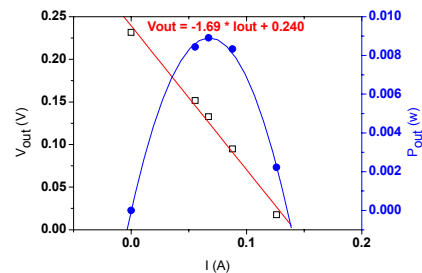


Figure 6: V_{out} versus I_{out} and P_{out} for the unileg In_2O_3 type device

The R_{int} resistances reach 6.36Ω , 4.1Ω and 1.69Ω respectively in the PN device (36 legs, $3 \times 3 \times 10 \text{ mm}^3$), the $\text{Ca}_{0.95}\text{Sm}_{0.05}\text{MnO}_3$ -based (36 legs, $3 \times 3 \times 10 \text{ mm}^3$) and the $\text{In}_{1.94}\text{Ge}_{0.06}\text{O}_3$ -based (16 legs, $5 \times 5 \times 5 \text{ mm}^3$)

unileg devices. The extracted contact resistances present values of 0.83Ω , 2Ω and 1.5Ω , respectively. Considering the different leg numbers and the different leg sections, to simplify the comparison, we can introduce the electrical contact resistivity ρ_c ($m\Omega.cm^2$) defined as the product of one contact resistance value with the section of the contact. In this context, values of 2.25, 5.14 and $11.72 m\Omega.cm^2$ are obtained respectively for the PN module, the $Ca_{0.95}Sm_{0.05}MnO_3$ -based and the $In_{1.94}Ge_{0.06}O_3$ -based unileg devices. This observation shows the contact quality varies with the used compound and is very large for the $In_{1.94}Ge_{0.06}O_3$ oxide. For the two other compounds lower values are obtained but the contacts qualities are hardly reliable. The other interesting point concerns the temperatures gradient measured on the devices. In the unileg architecture, the risk of thermal short circuit is evident, since Ag-foils go from top to bottom legs. To build N-type unileg modules, the P-type material has been substituted by respectively, Ag-wire of 0.125 mm diameter for the $Ca_{0.95}Sm_{0.05}MnO_3$ -based device and by Ag-foil for the $In_{1.94}Ge_{0.06}O_3$ device. For these two materials, the difference of thermal conductivity varies by 4 orders of magnitude and the electrical resistivity by 10. Then, by reducing the Ag section the risk of thermal short circuit can be avoided. Although the temperature differences are lower in the unileg device than in the conventional device, a value of 360 K is reached for the $Ca_{0.95}Sm_{0.05}MnO_3$ -based device and allows obtaining the same maximum output power value of $270mW$ than the PN device which presents a temperature difference of $460K$. For the $In_{1.94}Ge_{0.06}O_3$ device, the large section of the Ag-foils ($2mm$ width) and the smaller bars, conduct to an observed thermal short circuit (temperature difference of only 200 K). Finally, looking on the efficiency of such devices, defined as the ratio between heat input and power output, the two 36-legs modules exhibit

similar values around 0.48% (PN) and 0.6% (unileg). These low calculated values are of course related to high electrical contact resistances.

Conclusion

In conclusion, the unileg architecture leads to functional module when using Ag-threads. The 36-legs unileg device can generate 270 mW with a temperature difference of 360 K and a hot module temperature of 710 K, a value similar to the conventional PN device one, but for lower temperature difference and T_{hot} temperature. The possibility to keep only the best material is a real advantage of unileg assemblies. Nevertheless, it appears that the electrical contact resistances strongly reduce the devices performances. For the same gradient, with low contact resistances, it is expected to get an output power of 540 mW. In addition, with a larger gradient of 663 K, output power of $1.8W$ could be reached. Therefore, it seems to be necessary to investigate deeply the fabrication process. A new way to prepare and improve the contact resistance is underway.

References:

- [1] K. Fujita, K. Nakamura, and H. Yakabe in *Oxide Thermoelectrics*, edited by K. Koumoto (Research Signpost, Trivandrum, 2002).
- [2] S. Isobe, T. Tani, Y. Masuda, W. Seo, and K. Koumoto, *Jpn. J. Appl. Phys.* 41, 731 (2002).
- [3] M. Mikami, R. Funahashi, M. Yoshimura, Y. Mon, and T. Sasaki, *J. Appl. Phys.* 94, 10 (2003).
- [4] M. Ohtaki, T. Tsubota, K. Egushi, and H. Arai, *J. Appl. Phys.* 79, 1816 (1996).
- [5] D. Flahaut, T. Mihara and R. Funahashi, N. Nabeshima, K. Lee, H. Ohta and K. Koumoto, *J. Appl. Phys.*, 100, 084911 (2006).
- [6] D. Berardan, E. Guilmeau, A. Maignan, B. Raveau, *Solid State Comm.*, 146, 97-101 (2008)
- [7] A. C. Masset, C. Michel, A. Maignan, M. Hervieu, O. Toulemonde, F. Studer, and B. Raveau, *Phys. Rev. B*, 62, (2000)
- [8] W. Shin, N. Murayama, K. Ikeda, S. Sago, *Journal of Power Sources*, 103, 80-85 (2001)
- [9] R. Funahashi, M. Mikami, T. Mihara, S. Urata, N. Ando, *J. Appl. Phys.*, 99, 066117 (2006)
- [10] I. Matsubara, R. Funahashi, T. Takeuchi, S. Li, K. Ueno, S. Sodeoka, Proceeding ICT (2000)
- [11] R. Funahashi, T. Mihara, M. Mikami, S. Urata, N. Ando, E. Guilmeau, Proceeding ETS (2004)
- [12] R. Funahashi, S. Urata, K. Mizuno, T. Kouuchi, M. Mikami, *Appl. Phys. Lett.*, 85, (2004)
- [13] E. Sudhakar Reddy, J. G. Noudem, S. Hebert, C. Goupil, *J. Phys. D: Appl. Phys.*, 38, 3751-3755, (2005)
- [14] R. Funahashi, M. Mikami, S. Urata, M. Kitawaki, T. Kouuchi, K. Mizuno, *Meas. Sci. Technol.*, 16, 70-80, (2005)
- [15] Y. Zhang, J. Zhang, Q. Lu, *Ceramics International*, 33, (2007) 1305-1308